

EVIDENCE FOR A $T = 0$ THREE PION RESONANCE AT $M \sim 990$ MeV*

by

G.B. Chadwick, Z.G.T. Guiragossian, E. Pickup
Stanford Linear Accelerator Center, Stanford, California

and

A. Barbaro-Galtieri, M.J. Matison, A. Rittenberg
Lawrence Radiation Laboratory, Berkeley, California

In a study of the reaction $K^- n \rightarrow \Sigma^- \pi^+ \pi^- \pi^0$ from an exposure of 2.1 and 2.65 GeV/c K^- meson in the LRL 72" deuterium bubble chamber, we find evidence for a resonance in the neutral 3π system at 990 MeV. We are able to estimate our experimental resolution from the observed width of ω^0 . We find that an upper limit on the true width of this state is $\Gamma^{\text{true}} \leq 55$ MeV. We tentatively identify this state as having the same properties as the H-meson.^{1, 2}

The experiment and its interpretation are complicated by the well known difficulties associated with deuterium and Σ^- events, and by the extraordinary number of reported boson resonances around 1 GeV. We believe we have resolved the first mentioned difficulties by subjecting each of the 5822 analysed events at both energies to a critical examination at the scanning table, for ionization and general credibility.

Figure 1 (c, d) shows the 3π invariant mass distributions for this reaction at the two energies. The shaded histogram represents events with squared momentum transfer to the Σ^- less than $0.6 \text{ GeV}/c^2$. In the 2.1 GeV/c data a clear peak at ~ 990 MeV is apparent along with the η^0 and ω^0 signals, even in the total sample, while at 2.65 GeV/c it becomes significant only at low

* Work supported by the U. S. Atomic Energy Commission.

(Submitted to the Heidelberg International Conference on Elementary Particles, September 20-27, 1967.)

momentum transfers. Figure 1 (a,b) shows Chew Low plots of the data, in which the clustering of points at low momentum transfers is apparent.

We have considered what instrumental biases could produce this effect. In Fig. 2 we show the results of one test. If badly measured, three-body events had crept into the sample we would expect low laboratory energy π^0 's to appear. A comparison, especially of ω and H associated events, shows no qualitative difference. We also find the Σ^- lifetime well reproduced except for some loss of long lived Σ^- 's. However, events with long lived Σ^- 's show a 3π mass distribution similar to that of the total sample.

The effects of reflection of Y^* resonance on the 3π mass spectrum have been studied with the aid of the FORTRAN program MURTLBERT.³ This program simultaneously fits Breit-Wigner curves in all channels. The small contribution of Y^* resonances in this reaction accounts for the absence of serious reflections in the backgrounds of Fig. 1 (c, d).

The isotopic spin of this resonance may be found from a consideration of the possible reaction

$$K^- n \rightarrow \Sigma^0 H^- .$$

Since the $K^- n$ system is a pure $I = 1$ state, this reaction should have the same intensity as $K^- n \rightarrow \Sigma^- H^0$ if $I_H = 1$. In the worst case, an $I = 1$ 3π state would then satisfy the following condition:

$$R = \frac{K^- n \rightarrow \Sigma^0 H^-; H^- \rightarrow \pi^+ \pi^- \pi^-}{K^- n \rightarrow \Sigma^- H^0; H^0 \rightarrow \pi^+ \pi^0 \pi^-} \geq 0.5 .$$

Similarly, R would have the value 1.5 if $I_H = 2$. We have examined the $\pi^+ \pi^- \pi^-$ spectrum from the reaction $K^- n \rightarrow \Sigma^0 \pi^+ \pi^- \pi^-$, and find no signal. If $R \geq 0.5$, then the probability of observing no signal is less than 1/400. This indicates the $I = 0$ assignment to the resonance.

We now discuss why the interpretation of this effect excludes other known resonances in this region:

1. ϕ^0 meson: The branching ratio of $\phi^0 \rightarrow 3\pi$ can be taken to be $12 \pm 4\%$. we have considered the possible confusion of K^+ and K^- in the $\pi^+\pi^-$ tracks, and the resultant contamination of $K^-n \rightarrow \Sigma^- \phi^0$, $\phi^0 \rightarrow K^+K^-$. Based upon $8 \pm 3 \mu b$ cross section of $K^-p \rightarrow \Sigma^0 \phi$, $\phi \rightarrow K^+K^-$, and the number of events which could result in the K/π ambiguity, we find that the effect of such a confusion is negligible at our H peak.

2. δ -meson: The effect at mass ~ 965 MeV observed by Kienzle et al.,⁵ Allen et al.,⁶ Oostens et al.,⁷ have charged modes. Our isotopic spin assignment rules out this explanation.

3. A_1 meson: Ruled out on isotopic spin.

4. η' meson: In the mode

$$\eta' \rightarrow \pi^+ \pi^- \gamma$$

the γ can be fitted easily as a π^0 . In the missing mass events, however, we observe a peak at the η^0 mass, corresponding to the decay of

$$\eta' \rightarrow \eta^0 \pi^+ \pi^- .$$

Using the branching ratio

$$\frac{\eta' \rightarrow \pi^+ \pi^- \gamma}{\eta' \rightarrow \pi^+ \pi^- \eta} = 25 \pm 3\% \quad 8$$

at 2.1 GeV/c, we expect $18 \pm 5 \eta' \rightarrow \pi^+ \pi^- \gamma$ events on the lower side of the 990 MeV mass region - only 25% of the observed signal. But the 2.65 GeV/c data may not be so clearly defined. It is possible that half of the 990 MeV peak observed at low momentum transfers, can be accounted for by the expected $7 \pm 3 \eta' \rightarrow \pi^+ \pi^- \gamma$ events; although this would assume a shift of 30 MeV in the η' mass. This 7 ± 3 events was calculated with the same momentum transfer cut of $t(n, \Sigma^-) < 0.6 \text{ GeV}/c^2$.

Properties of the H

A Dalitz plot of the mass region $0.94 < M(3\pi) < 1.02$ GeV is shown in Fig. 3. It should be noted that in this mass region the Dalitz plot area would be almost entirely covered by ρ meson bands. So that without very large statistics it would be impossible to prove any ρ association. Thus, we cannot confirm the $\rho\pi$ decay mode as suggested by Bartsch et al.,¹ and by Benson et al.²

In Fig. 4 we have plotted the number of events in the Dalitz plot against equal areas defined by the variable

$$\lambda = \left| \vec{p}_1 \times \vec{p}_2 \right| / \left| (\vec{p}_1 \times \vec{p}_2)_{\max} \right| .$$

There is a fall-off toward the edges of the plot where λ goes to zero, which is common to H, ω , and background. Such a term would arise for the spin series 1^- , 2^+ , etc. However, we are unable to accurately determine the background behavior, and thus cannot rule out a 1^+ spin interpretation.^{1,2}

Further evidence for non-zero spin is obtained from the angular correlations. Figure 5 shows the Trieman Yang, Stapp and Jackson angular distributions for the H and for the ω . All show some correlations which will rule out zero spin. The interpretation of these data, however, is complicated by s-channel effects, as is illustrated in Fig. 6 where the center-of-mass angular distributions for ω and H are shown. Evidence for a backward, as well as forward, meson peaking is strong in the 2.1 GeV/c data. Here, the beam energy is very close to a resonance found in the K^-p total cross section at mass 2260 MeV.^{9*} We shall continue a study of these processes.

In conclusion, Table I summarizes the several channel cross sections and resonance parameters. The Y^* states are discussed in a separate paper.¹⁰

* For comparison Fig. 6(e, f) shows the ρ^0 center-of-mass angular distributions from the reaction $K^-n \rightarrow \Sigma^- \pi^+ \pi^-$.

REFERENCES

1. J. Bartsch et al., ABBBHLM collaboration, Phys. Letters 11, 167 (1964).
2. G. Benson, E. Marquit, B. Roe, D. Sinclair and J. Vander Velde, Phys. Rev. Letters 17, 1234 (1966).
3. J. Friedman, Lawrence Radiation Laboratory Document APG Note P-156, (1966).
4. J. S. Lindsey and G. A. Smith, Phys. Letters 20, 93 (1966).
5. W. Kienzle, B. C. Maglic, B. Levrat, F. Lefebvres, D. Freytag and H. R. Blieden, Phys. Letters 19, 438 (1965).
6. D. D. Allen, G. P. Fisher, G. Godden, L. Marshall and R. Sears, Phys. Letters 22, 543 (1966).
7. J. Oostens, P. Chavanon, M. Crozon, and J. Tocqueville, Phys. Letters 22, 708 (1966).
8. G. R. Kalbfleisch, O. Dahl, A. Rittenberg, Phys. Rev. Letters 13, 349a (1964) and P. M. Dauber, N. E. Slater, L. T. Smith, D. H. Stork, and H. R. Ticho, Phys. Rev. Letters 13, 449 (1964).
9. Cool, et al., Phys. Rev. Letters 16, 1228 (1966).
10. G. B. Chadwick, Z.G.T. Guiragossian, E. Pickup, A. Barbaro-Galtieri, M. J. Matison, and A. Rittenberg, Stanford Linear Accelerator Center Document SLAC PUB-348, September (1967).

TABLE I

Channel cross sections and resonance
parameters in $K^-n \rightarrow \Sigma^- \pi^+ \pi^0 \pi^- [p]$

 $\sigma \mu b$

| 2.1 GeV/c, $K^-n \rightarrow \Sigma^- \pi^+ \pi^0 \pi^-$ | | | | 312 |
|---|--------|----------------|-----------------------|--------------|
| Channel Parameters from MURTLBERT Fit | | | | |
| | M, MeV | Γ , MeV | Amount from fit, % | |
| $K^-n \rightarrow \Sigma^- \eta^0$ | 548 | 50 | 4.4 ± 1.0 | 14 ± 3 |
| $\rightarrow \Sigma^- \omega^0$ | 783 | 60 | 37.7 ± 3.3 | 118 ± 40 |
| $\rightarrow \Sigma^- H^0$ | 996 | 80 | 12.0 ± 3.7 | 37 ± 11 |
| $\rightarrow \Sigma^- \pi^0 \rho^0$ | 760 | 100 | 4.3 ± 2.0 | 14 ± 6 |
| $\rightarrow Y_1^* \pi^+ \pi^-$ | 1390 | 50 | 14.4 ± 3.0 | 45 ± 9 |
| $\quad \hookrightarrow \Sigma^- \pi^0$ | | | | |
| $\rightarrow Y_1^* \pi^- \pi^0$ | 1385 | 35 | ~ 3 | ~ 9 |
| $\rightarrow Y_0^* \pi^- \pi^0$ | 1408 | 25 | 5.5 ± 2.0 | 17 ± 6 |
| $\rightarrow Y_0^* \pi^- \pi^0$ | 1520 | 25 | 4.7 ± 2.0 | 15 ± 6 |
| $\rightarrow Y_{0,1}^* \pi^- \pi^0$ | 1660 | 45 | - | - |
| $\quad \hookrightarrow \Sigma^- \pi^+$ | | | | |
| 2.65 GeV/c, $K^-n \rightarrow \Sigma^- \pi^+ \pi^0 \pi^-$ | | | | 270 |
| $K^-n \rightarrow \Sigma^- \eta^0$ | 548 | 50 | 5.0 ± 0.6 | 13.5 ± 2 |
| $\rightarrow \Sigma^- \omega^0$ | 783 | 45 | 24.0 ± 1.0 | 65 ± 8 |
| $\rightarrow \Sigma^- H^0$ | 990 | | difficult to estimate | |
| $\rightarrow \Sigma^- \pi^0 \rho^0$ | 760 | 100 | 0 | |
| $\rightarrow Y_1^* \pi^+ \pi^-$ | 1385 | 35 | 13 ± 1.0 | 35 ± 5 |
| $\quad \hookrightarrow \Sigma^- \pi^0$ | | | | |
| $\rightarrow Y_0^* \pi^- \pi^0$ | 1405 | 30 | 3.5 ± 0.8 | 9 ± 3 |
| $\rightarrow Y_0^* \pi^- \pi^0$ | 1522 | 30 | 5 ± 1.0 | 13.5 ± 3 |
| $\rightarrow Y_{0,1}^* \pi^- \pi^0$ | 1660 | 45 | 5.8 ± 1.0 | 16 ± 3 |
| $\quad \hookrightarrow \Sigma^- \pi^+$ | | | | |

FIGURE CAPTIONS

1. (a) and (b) Chew Low scatter plots, (c) and (d) $(\pi^+ \pi^0 \pi^-)$ mass histograms, at 2.1 and 2.65 GeV/c, respectively. Shaded events with $t(n, \Sigma^-) < 0.6$ GeV/c².
2. π^0 laboratory momentum distributions at indicated $M(\pi^+ \pi^0 \pi^-)$ intervals. Unshaded histograms are from events with invisible spectator protons, shaded histograms with visible spectators.
3. Normalized $\pi^+ \pi^0 \pi^-$ Dalitz plots from data at 2.1 and 2.65 GeV/c with $t(n, \Sigma^-) < 0.6$ GeV/c². (a) at ω : $0.740 \leq m(\pi^+ \pi^0 \pi^-) \leq 0.840$ GeV, and (b) at H: $0.940 \leq m(\pi^+ \pi^0 \pi^-) \leq 1.020$ GeV.
4. Equal area radial density distributions in the $\pi^+ \pi^0 \pi^-$ Dalitz plots, from the combined data with momentum transfer cut at 0.6 GeV/c². For events in the H, ω and background regions.
5. Production and decay angular correlations (a-d) for ω , (e-h) for H, and (i-l) for background events. $\hat{n}_{3\pi}$ is the normal to the 3π decay plane evaluated in the 3π rest frame.
6. Center-of-mass production angular distribution (a, b) for ω^0 , (c, d) for H events, at 2.1 and 2.65 GeV/c, respectively. Compared with ρ^0 production in $K^- n \rightarrow \Sigma^- \pi^+ \pi^-$ in (e, f).

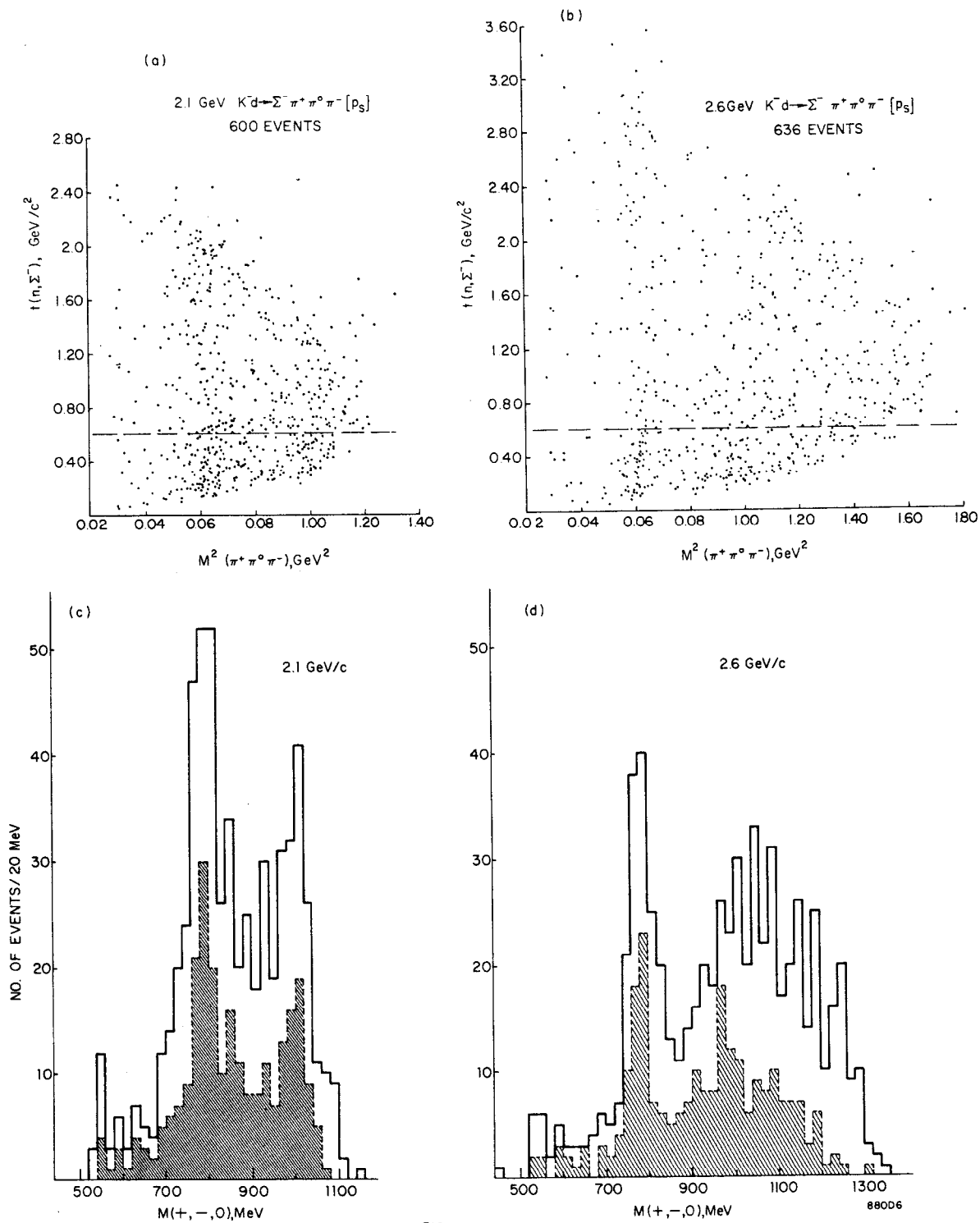


FIG.1

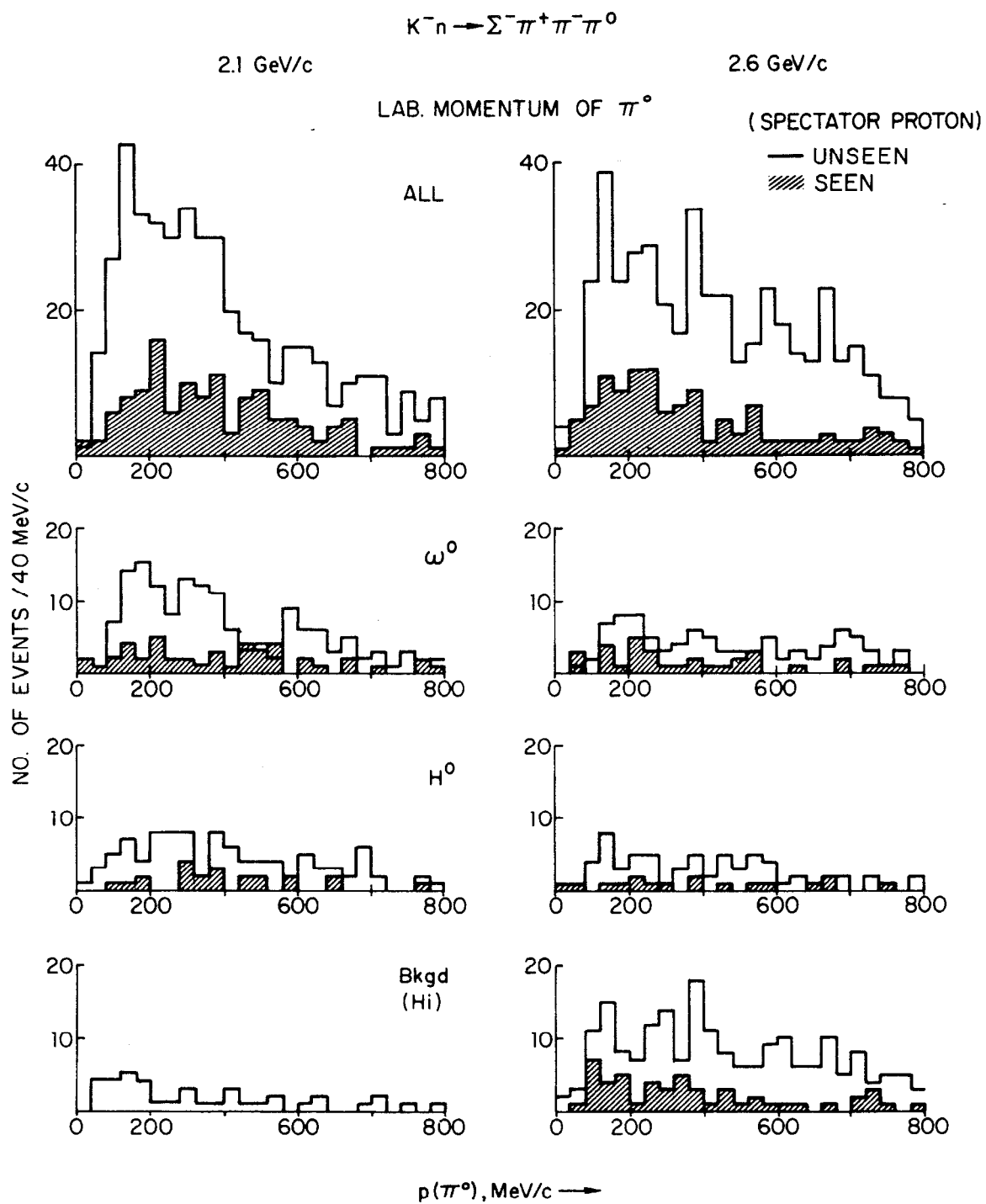


FIG. 2

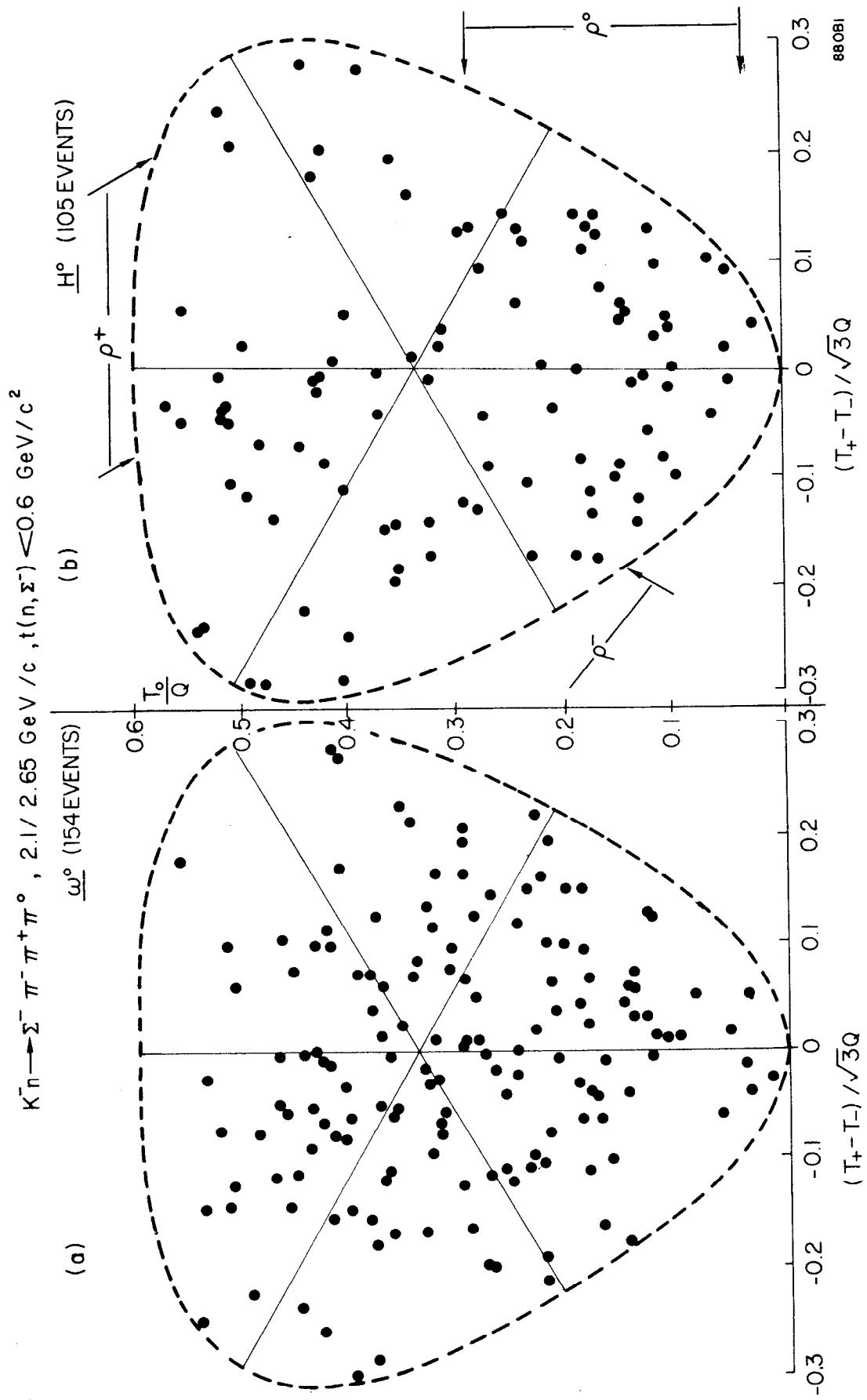


FIG. 3

RADIAL DENSITY DISTRIBUTION IN 3π DALITZ PLOTS

$K^-d \rightarrow \Sigma^- \pi^+ \pi^- \pi^0 (P_S), 2.1/2.65 \text{ GeV}/c, t(n, \Sigma^-) < \text{GeV}/c^2$

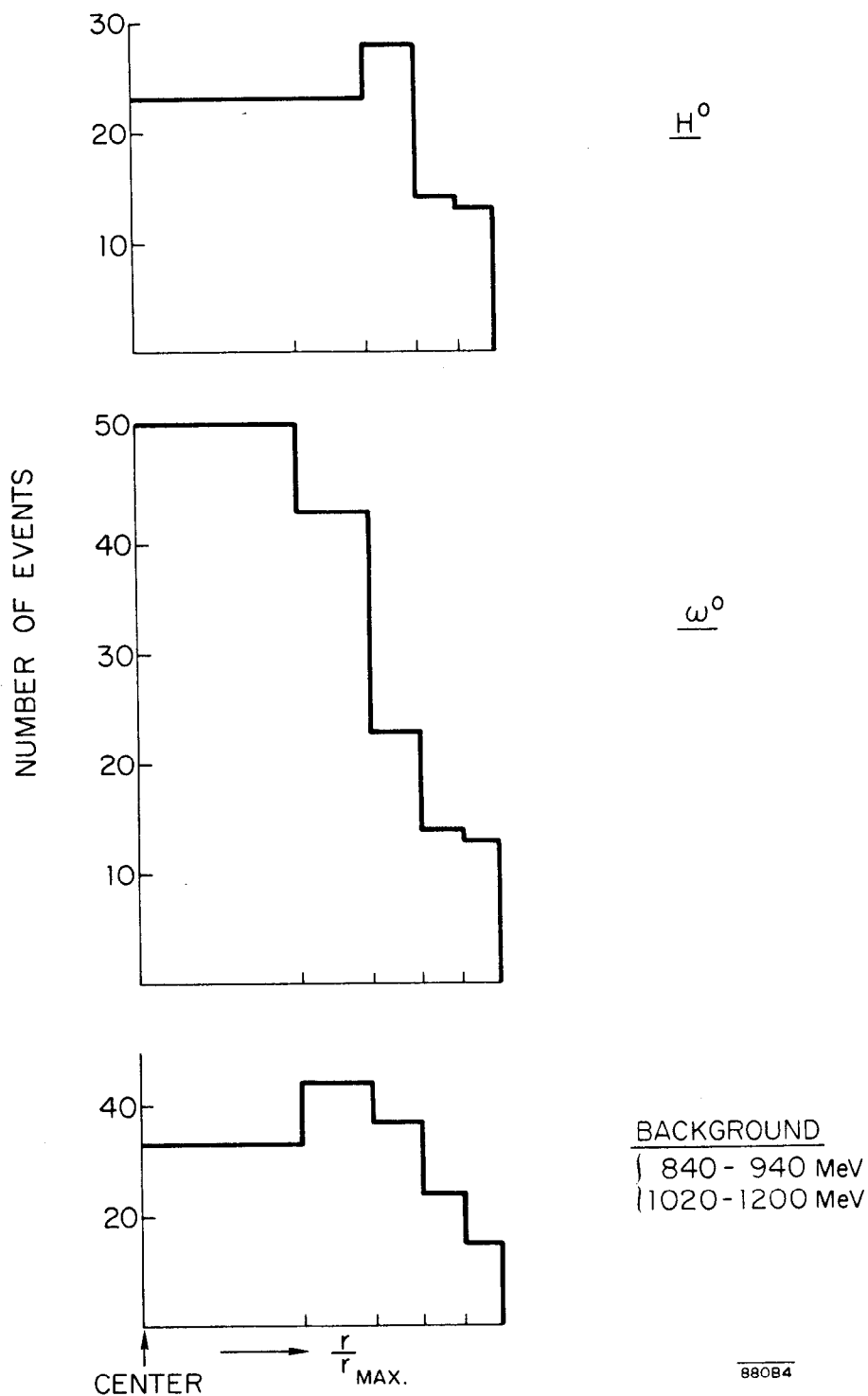
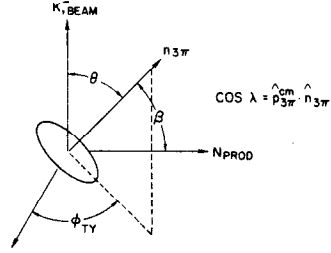


FIG 4

$K^- d \rightarrow \Sigma^- \pi^+ \pi^- \pi^0 (p_3), 2.1 \text{ AND } 2.65 \text{ GeV}/c$
 $t(n, \Sigma^-) < 0.6 \text{ GeV}/c^2$



$\omega : 0.740 \leq m(\pi^+ \pi^0 \pi^-) \leq 0.840 \text{ GeV}$
 $H : 0.940 \leq m(\pi^+ \pi^0 \pi^-) \leq 1.020 \text{ GeV}$
 $\text{BACKGROUND: } 0.840-0.940 \text{ OR } 1.020-1.200 \text{ GeV}$

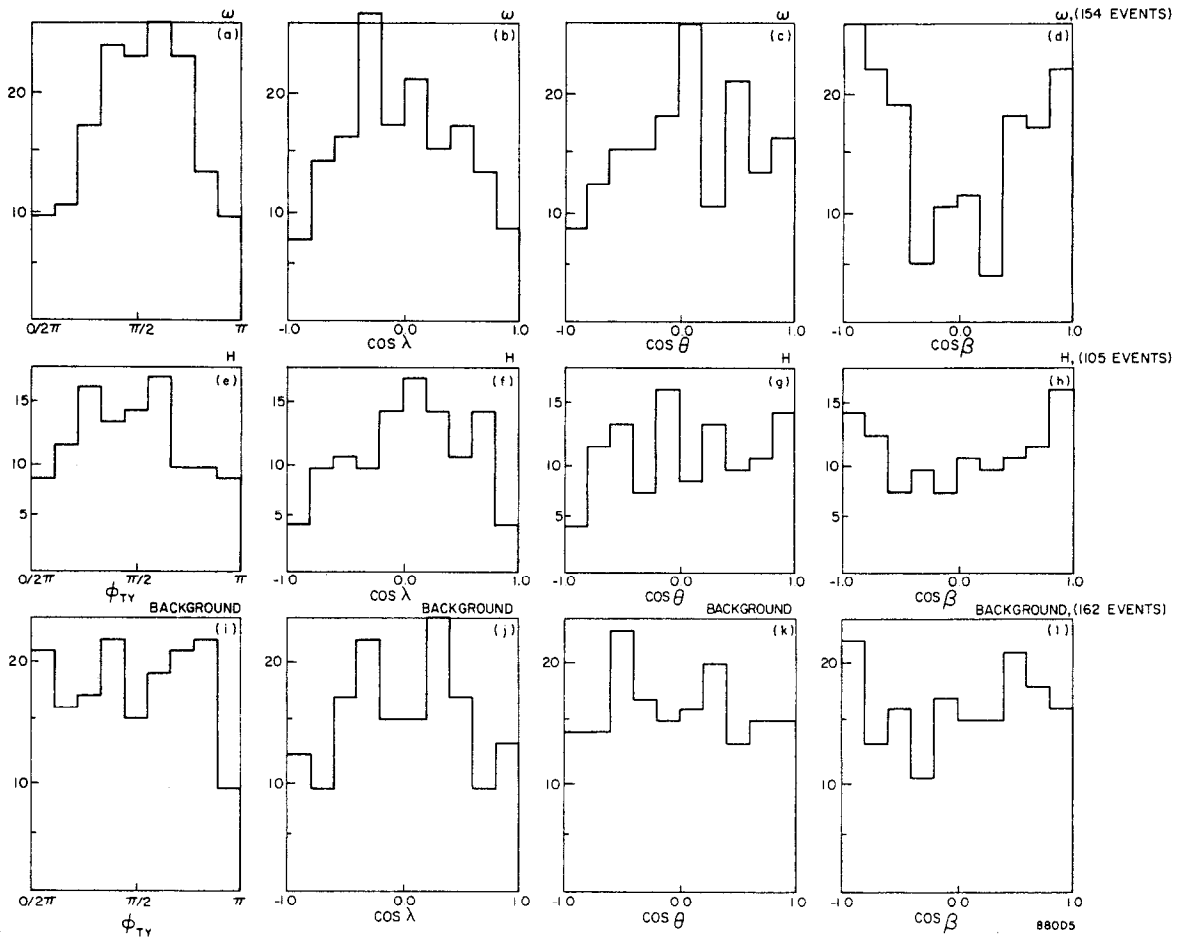


FIG 5

88005

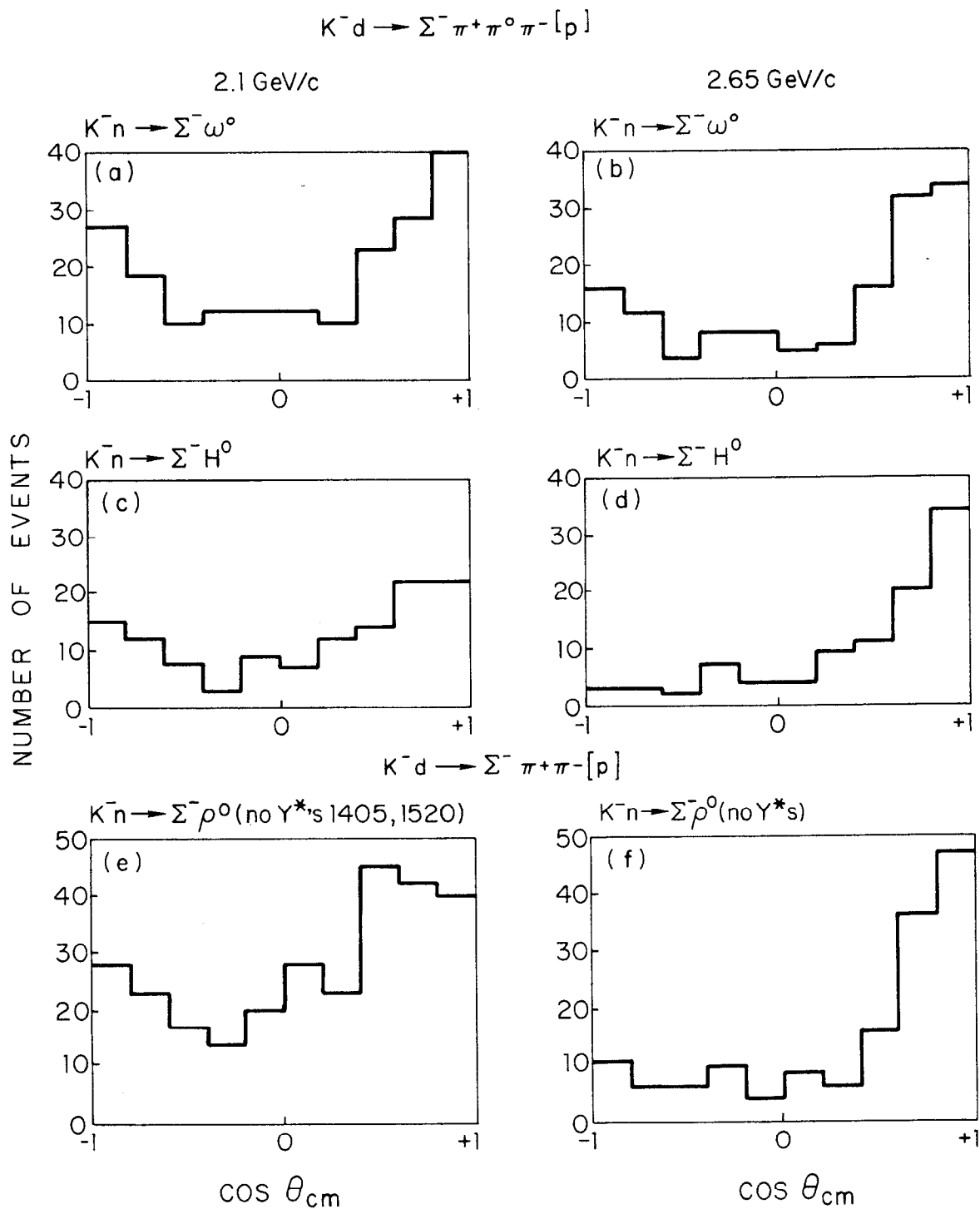


FIG. 6